

Stochastic Memristive Interface for Neural Signal Processing

Svetlana A. Gerasimova ^{1,2}, Alexey I. Belov ², Dmitry S. Korolev ², Davud V. Guseinov ², Albina V. Lebedeva ¹, Maria N. Koryazhkina ³, Alexey N. Mikhaylov ², Victor B. Kazantsev ^{1,4,5} and Alexander N. Pisarchik ^{3,4,6,*}

- ¹ Institute of Biology and Biomedicine, National Research Lobachevsky State University of Nizhny Novgorod, 603950 Nizhny Novgorod, Russia; gerasimova@neuro.nnov.ru (S.A.G.); lebedeva@neuro.nnov.ru (A.V.L.); kazantsev@neuro.nnov.ru (V.B.K.)
 - ² Research Institute and Technology, National Research Lobachevsky State University of Nizhny Novgorod, 603950 Nizhny Novgorod, Russia; belov@nifti.unn.ru (A.I.B.); dmkorolev@phys.unn.ru (D.S.K.); guseinov@phys.unn.ru (D.V.G.); mian@nifti.unn.ru (A.N.M.)
 - ³ Research and Educational Center “Physics of Solid State Nanostructures”, National Research Lobachevsky State University of Nizhny Novgorod, 603950 Nizhny Novgorod, Russia; mahavenok@mail.ru
 - ⁴ Laboratory of Neuroscience and Cognitive Technology, Innopolis University, 420500 Innopolis, Russia
 - ⁵ Center for Neurotechnology and Machine Learning, Immanuel Kant Baltic Federal University, 236016 Kaliningrad, Russia
 - ⁶ Center for Biomedical Technology, Universidad Politécnica de Madrid, Pozuelo de Alarcón, 28223 Madrid, Spain
- * Correspondence: alexander.pisarchik@ctb.upm.es

Abstract: We propose a memristive interface consisting of two FitzHugh–Nagumo electronic neurons connected via a metal–oxide (Au/Zr/ZrO₂(Y)/TiN/Ti) memristive synaptic device. We create a hardware–software complex based on a commercial data acquisition system, which records a signal generated by a presynaptic electronic neuron and transmits it to a postsynaptic neuron through the memristive device. We demonstrate, numerically and experimentally, complex dynamics, including chaos and different types of neural synchronization. The main advantages of our system over similar devices are its simplicity and real-time performance. A change in the amplitude of the presynaptic neurogenerator leads to the potentiation of the memristive device due to the self-tuning of its parameters. This provides an adaptive modulation of the postsynaptic neuron output. The developed memristive interface, due to its stochastic nature, simulates a real synaptic connection, which is very promising for neuroprosthetic applications.

Keywords: memristive device; neuron-like oscillator; stochastic dynamics; synchronization; neuromorphic circuit; FitzHugh–Nagumo neuron



Citation: Gerasimova, S.A.; Belov, A.I.; Korolev, D.S.; Guseinov, D.V.; Lebedeva, A.V.; Koryazhkina, M.N.; Mikhaylov, A.N.; Kazantsev, V.B.; Pisarchik, A.N. Stochastic Memristive Interface for Neural Signal Processing. *Sensors* **2021**, *21*, 5587. <https://doi.org/10.3390/s21165587>

Academic Editor: Manuel José Cabral dos Santos Reis

Received: 2 July 2021

Accepted: 16 August 2021

Published: 19 August 2021

Publisher’s Note: MDPI stays neutral with regard to jurisdictional claims in published maps and institutional affiliations.



Copyright: © 2021 by the authors. Licensee MDPI, Basel, Switzerland. This article is an open access article distributed under the terms and conditions of the Creative Commons Attribution (CC BY) license (<https://creativecommons.org/licenses/by/4.0/>).

1. Introduction

The design of compact neuromorphic systems, including micro- and nanochips, capable of reproducing information and computational functions of brain cells is a great challenge of modern science and technology. Such systems are of interest for both fundamental research in the field of nonlinear dynamics and the synchronization of complex systems [1–7], as well as medical applications in the devices for monitoring and stimulating brain activity in the framework of neuroprosthetic tasks [8–10]. Due to their importance, memristive devices have recently become the subject of intense research, especially in the area of neuromorphic and neurohybrid applications [11–17]. Neuromorphic technologies are especially relevant for intelligent adaptive automatic control systems—biorobots. It is also worth noting that the construction and creation of electronic neurons and synapses (connections between neurons) based on thin-film memristive nanostructures is a fast-growing area of interdisciplinary research in the development of neuromorphic systems [18–20].

The history of neuromorphic technologies began in the late 1980s with the emergence of computation machines, and since then, significant advances have been achieved in elec-

tronics, physics of micro- and nanostructures, and solid-state nanoelectronics. The careful development of neuron-like electrical circuits made it possible to reproduce basic neural behaviors, such as resting, spiking, and bursting dynamics, as well as more sophisticated regimes, including chaos and multistability [21–25].

A memristive device is usually based on the Chua's model [19], which is an element of an electrical circuit capable of changing resistance depending on an electrical signal entering its input. In recent decades, various thin-film memristive nanostructures have been created. They are capable of changing their conductivity under the action of a pulsed signal [26,27], which makes the memristor an almost ideal electronic analogue of a synapse [13]. A synapse is known to be a communication channel between neurons that provides unidirectional signal transmission from a transmitting (presynaptic) neuron to a receiving (postsynaptic) neuron. This communication channel ensures the propagation of a nerve impulse along the axon of the transmitting cell.

The synaptic communication results in synchronization of postsynaptic and presynaptic neurons. Neural synchronization was extensively studied using various mathematical models and described in terms of periodic solutions [3,6,28–35]. Such artificial synapses were implemented as electronic circuits that convert pulses of presynaptic voltage into postsynaptic currents with some synaptic amplification. Different strategies were used for the hardware implementation of synaptic circuits, e.g., an optical interface between electronic neurons [4,5,7].

Recent advances in nanotechnology allowed for miniaturization of artificial synapses by creating memristive nanostructures that mimic dynamics of real synapses. Among various candidates for the role of electronic synapses, memristive devices have a great potential for implementing massive parallelism and three-dimensional integration in order to achieve good efficiency per unit volume [36–38]. In this regard, it is important to create a memristor-based neuromorphic system capable of processing neuron-like signals.

Recently, the interaction between electronic neurons through a metal-oxide memristive device was successfully implemented in hardware [39]. The prerequisite for such a device was the study of the interaction of Van der Pol generators via a memristor [40]. Later, a significant effort was invested in theoretical research to study synchronization between neuron-like generators connected through a memristive device [14,41]. However, to the best of our knowledge, experimental studies of the dynamics of FitzHugh–Nagumo (FHN) neurons connected by a memristive synapse have not yet been carried out. We believe that the creation of neuromorphic memristive systems will lead to the production of simple and compact neuroelements based on memristive devices capable of imitating the electrophysiological behavior of real neurons.

At the same time, a memristive device made of metal oxides is of interest not only for experimental research, but also for theoretical studies. Neuromemristive models were found to exhibit complex dynamics, including chaos and chimeras [42,43], the study of which can contribute to the fundamental theory. On the other hand, many theoretical "memristive" neural models reported in the literature have nothing to do with the concept of memristive elements [44]. Therefore, the development of adequate mathematical models that can simulate real laboratory neuromemristive experiments is an actual problem.

Summarizing all the above, significant theoretical investigations of memristors and the possibility of their use as a part of neuromorphic systems were performed. In particular, not only dynamical effects were simulated, but also the simplest learning rules were implemented [45–52]. Currently, technologies are being developed to improve the characteristics of memristive devices in order to create reliable memristive networks capable of solving some mathematical tasks [53], classifying images [54–58], etc. [59–61]. Despite impressive theoretical results in the development of neuromorphic memristive systems, the experimental research of laboratory memristive devices, rather than their substitutes based on transistors or resistors as parts of dynamical systems, was not carried out because of high complexity of this task, which requires the cooperation of nanotechnologists, physicists, and neuroscientists.

In this work, we experimentally implement a memristive interface based on the metal–oxide nanostructure that acts as a synaptic interface connecting two electronic FHN neural generators. The interface allows for the analog simulation of the adaptive behavior and neural timing effects, which can be associated with synaptic plasticity. We also investigate the stochastic properties of the memristive device. For the first time, to the best of our knowledge, we perform an experimental study on such a memristive neural system and compare experimental results with numerical simulations.

2. Materials and Methods

In order to simulate neural dynamics, we explored two FHN neuron generators with cubic nonlinearity constructed using diodes [7,22]. The dynamics of the presynaptic FHN neuron was modeled by the normalized equations obtained with the Kirchhoff law [21] as follows:

$$\begin{aligned}\frac{du_1}{dt} &= f(u_1) - v_1 \\ \frac{dv_1}{dt} &= \varepsilon(g(u_1) - v_1) - I_1\end{aligned}\quad (1)$$

where u_1 is the membrane potential of the presynaptic neuron, v_1 is the “recovery” variable related to the ion current, $f(u_1) = u_1 - u_1^3/3$ is the cubic nonlinearity, I_1 is the depolarization parameter characterizing the excitation threshold, and ε is a small coefficient. If $u_1 < 0$, the function $g(u_1) = \alpha u_1$, and if $u_1 \geq 0$, $g(u_1) = \beta u_1$ (α, β being the parameters that control, respectively, the shape and location of the v -nullcline [22]).

The memristive device model was developed based on a standard approach to reflect the dynamical response of a memristor to electrical stimulation. The model describes a change in resistance, similar to potentiation and depression, based on physical laws identified in experiments [62]. The memristor model is given by the complex function:

$$\begin{aligned}j &= w j_{lin} + (1 - w) j_{nonlin} \\ j_{lin} &= u_1 / \rho \\ j_{nonlin} &= u_1 \exp(b\sqrt{u_1} - E_b) \\ w(u_1) &= A \exp\left(-\frac{E_m - \alpha_1 u_1}{kT}\right)\end{aligned}\quad (2)$$

This approach supposes the introduction of internal state variable w , which is determined by the fraction of the insulator region occupied by filaments. The change in this state is associated with the processes of migration of oxygen ions (vacancies) with the height of the effective migration barrier E_m . In turn, the migration is provided by the Joule heating kT and applied electric voltage u_1 . The total current density j through the memristor is the sum of the linear j_{lin} and nonlinear j_{nonlin} components. The former corresponds to ohmic conductivity with resistivity ρ , whereas the latter is determined by the transport of charge carriers through defects in the regions of the insulator not occupied by filaments (including those in the filament rupture region). It was previously found that, in the insulating state of the studied ZrO₂-based memristive devices, the current transport is implemented by the Poole–Frenkel mechanism with an effective barrier E_b [62]. The smooth transition between high- and low-resistance states (HRS and LRS, correspondingly) is determined by the dynamic contribution to the total current of the conductive filaments and, therefore, the state variable. In Equation (2), b , α_1 , and A are coefficients derived from experimental data. In our numerical simulations we used the Runge–Kutta integration methods for stochastic differential equations in Matlab [63–65].

In order to compare the experimentally observed dynamics of the memristive device with the results of numerical simulations, we needed to take into account stochasticity of microscopic processes leading to a change in the internal state w of the dynamical system. Random fluctuations of the normal distribution were added to energy barrier E_m for ion hopping (dispersion 10%), energy barrier E_b for electron jumps in the Poole–Frenkel conduction mechanism in the HRS (dispersion 1%), and ohmic resistance ρ of the structure in the LRS (dispersion 10%). This led to the scattering of the experimental current–voltage characteristics. The finite spread of the switching voltages is mainly related

to the stochasticity of the energy barrier for ions, whereas the change in the resistive states from cycle to cycle is associated with the electron transport stochasticity.

One-way communication between two neurons through the memristive device was modeled by the following equations:

$$\begin{aligned} \frac{du_1}{dt} &= f(u_1) - v_1 \\ \frac{dv_1}{dt} &= \varepsilon_1(g(u_1) - v_1) - I_1 \\ \frac{du_2}{dt} &= f(u_2) - v_2 + j(u_1)Sd \\ \frac{dv_2}{dt} &= \varepsilon_2(g(u_2) - v_2) - I_2 \end{aligned} \quad (3)$$

where d is the equivalent load resistance, $j(u_1)$ is the current density through the memristive device, S is the area of conductive filaments obtained from the experiment, and ε is a small recovery parameter. The signal from the presynaptic neural generator (u_1) was sent to the postsynaptic neural generator (u_2) through the memristive device.

Thus, the two neurogenerators were connected in such a way that part of the current $j(u_1)$ generated by the presynaptic neuron passed through the load resistor, which was connected in series with the memristive device, before reaching the postsynaptic neuron. The initial conditions and model parameters corresponded to the experimental conditions. In particular, both neural oscillators were initially in a self-oscillatory regime.

The designed neuromorphic circuit consisted of an FHN electronic circuit, a memristive device formed by the thin-film metal–oxide–metal nanostructure based on yttria-stabilized zirconia (Au/Zr/ZrO₂(Y)/TiN/Ti) [66], and a load resistor (Figure 1a). This memristive interface operated as follows. The electronic FHN neuron generated a pulse signal that affects the memristive device and thus modulates the oxidation and recovery of conductive filaments in the oxide film of the memristive device. The analog electronic FHN neuron consisted of the following blocks: an oscillatory contour unit, a nonlinearity unit, and an amplifier unit (see Figure 1b). The detailed design of this device is described in [7,22]. The FHN neural generator demonstrates the main qualitative features of neurodynamics: the presence of an excitability threshold and the existence of resting and spiking regimes. These regimes were controlled using a potentiometer. The spiking frequency was varied in the range of 10–150 Hz, the spike duration in the range of 10–25 ms, and the spike amplitude u_1 in the range of 1–6 V.

In this work, we used the National Instruments USB-6212 data acquisition system, which consists of a digital-to-analog converter (DAC) and two analog-to-digital converters (ADC). The data acquisition system was controlled using LabVIEW software. The pre-recorded neuron-like signal was applied to a memristive device with a sampling frequency of 5 kHz via the DAC. The ADCs recorded the voltage drop across the memristive device and the load resistor, which made it possible to calculate the memristive device resistance in real time. The potential difference across the memristive device (R_m) and the load resistor (R_2) was digitized at a sampling frequency of 10 kHz. Matlab was used to analyze the results.

After testing and tuning, the neuron-like oscillators were connected through the memristive device. Both analog neurogenerators were turned in the oscillatory regime. Under the neuron-like signal action, the memristive device changed its state from high resistive to low resistive. The amplitude of the presynaptic neuron was adjusted by the potentiometer in order to obtain a frequency-locking regime between two oscillators.

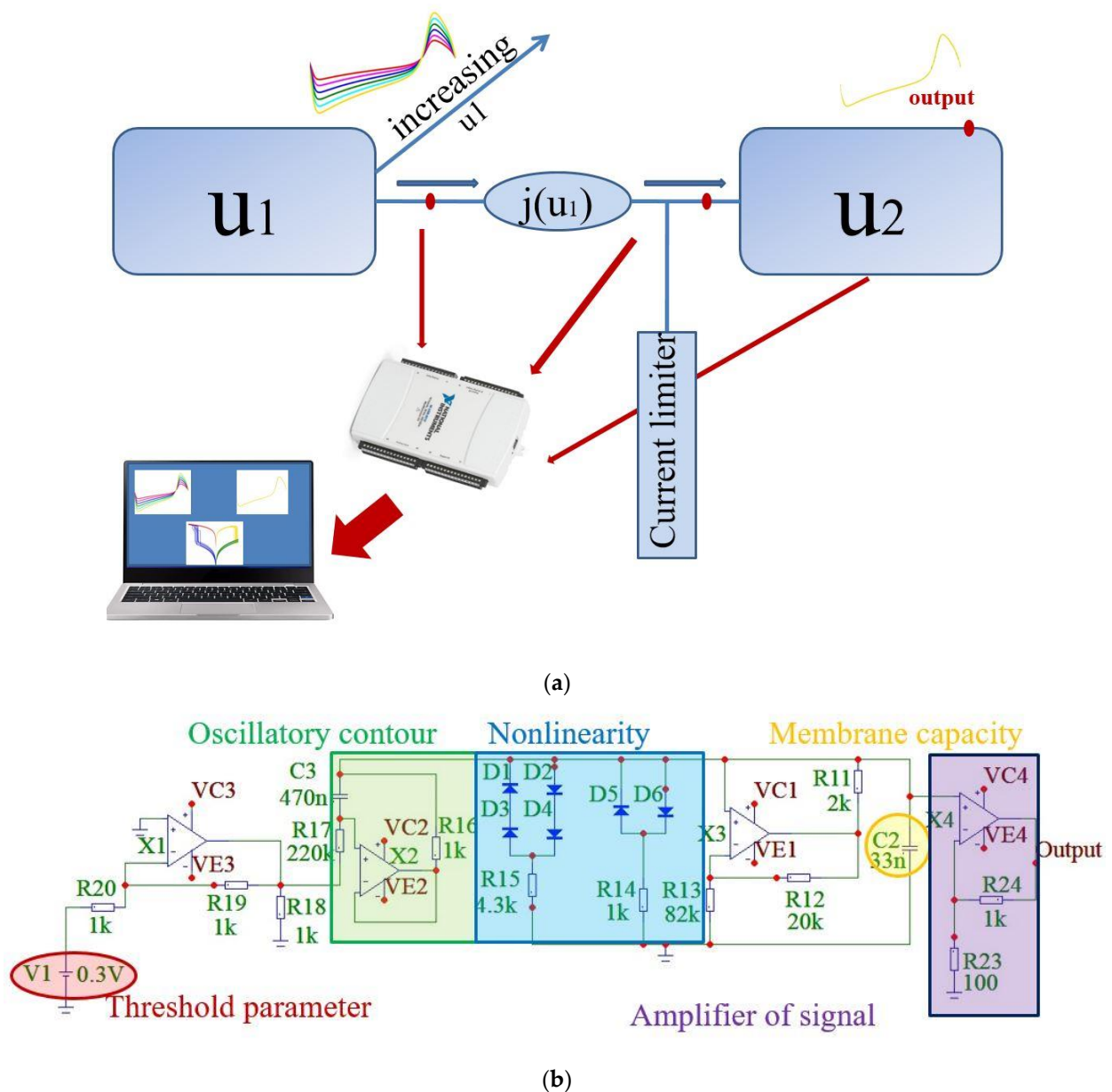


Figure 1. The system description: (a) block diagram of the interaction between presynaptic (u_1) and postsynaptic (u_2) electronic neurons through a memristive device. The neurons are initially in an oscillatory regime. The output of the presynaptic neuron is increased during the experiment; (b) analog electrical circuit of the FitzHugh–Nagumo neuron. The inductance is implemented by the circuit with operational amplifier, cubic nonlinearity is set using diodes D1–D6, capacitor C2 is related to the capacitance of the neuron membrane, and potential V1 is associated with an equilibrium controlled by the power source.

3. Results and Discussion

The output signal of the presynaptic electronic neuron is shown in Figure 2a. This signal is applied to the memristive device. The used neuron-like signal (u_1) is asymmetric (the minimum voltage is -5 V and the maximum voltage is 4 V) due to the asymmetry of the current–voltage characteristic (I – V curves) of the memristive device. For a more detailed study of the effect of the neuron-like signal on the memristive device, the curve in Figure 2a is visually divided into four intervals with different colors. Each interval corresponds to a specific fragment of the I – V curves in Figure 2b. The I – V curves in Figure 2b display the switching between LRS and HRS. The RESET process (switching from LRS to HRS) occurs with a positive voltage and SET (switching from HRS to LRS) with a negative voltage. The

scattering of the I - V curves in Figure 2b results from random fluctuations applied to the memristor parameters E_m , E_b , and ρ . Figure 2c demonstrates the increase in the amplitude of the presynaptic neuron from 1.558 V to 4 V. Figure 2d shows that, even when exposed to a small amplitude signal of 2 V (purple curve), the memristive device can switch from HRS to LRS.

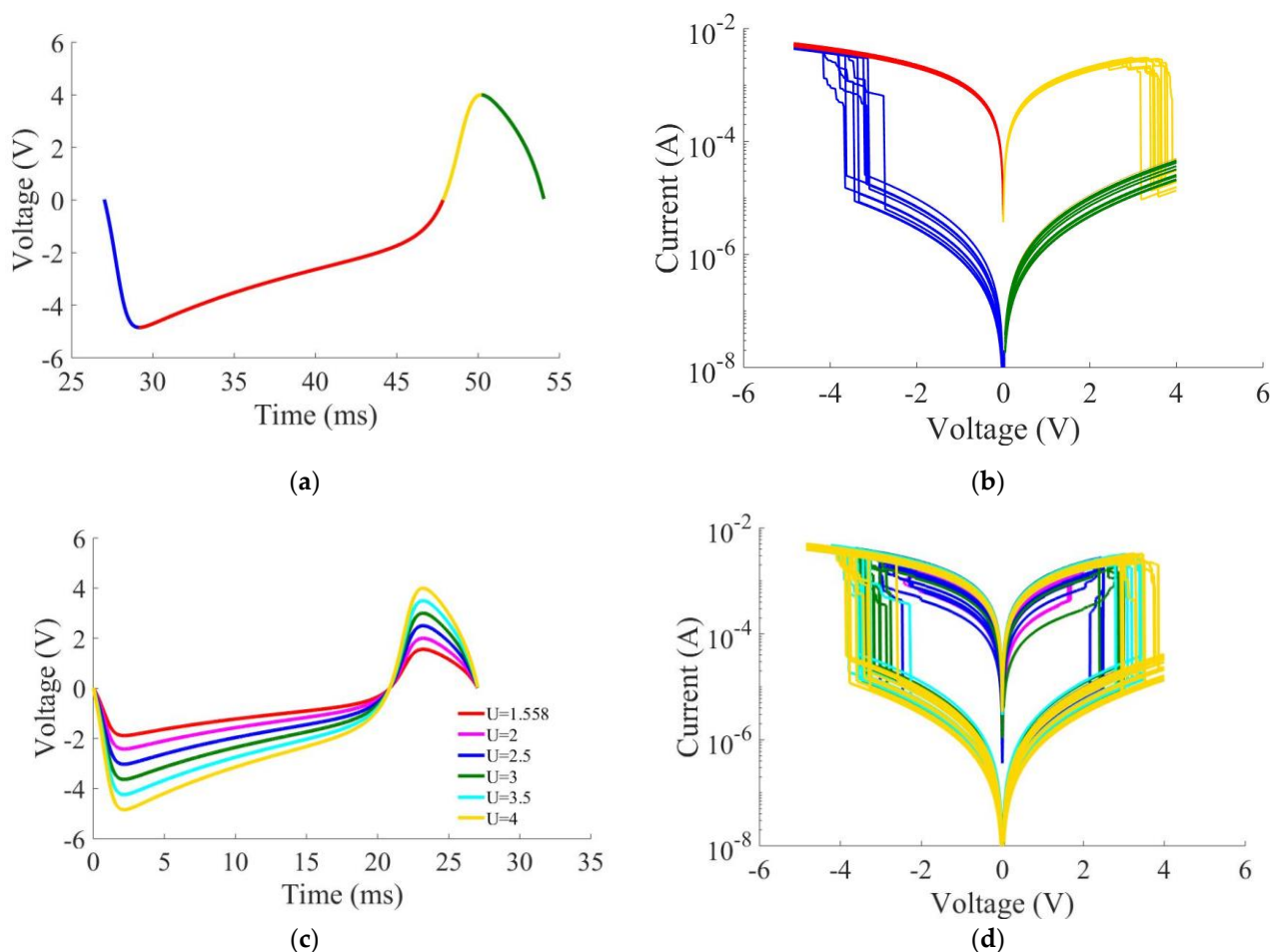


Figure 2. Experimental resistive switching in the response to a neuron-like signal: (a) neural-like pulse. The blue, red, yellow, and green colors show, respectively, the curve segments increasing from 0 to -5 V, from -5 to 0 V, from 0 to 4 V, and 4 to 0; (b) I - V curves. Each colored I - V section corresponds to a colored section of the input signal to memristor; (c) increasing amplitude of the neuron-like signal. The red, purple, blue, green, light blue, and yellow curve corresponds, respectively, to the peak amplitude of 1.558 V, 2 V, 2.5 V, 3 V, 3.5 V, and 4 V; (d) resistive switching of the memristive device under the action of corresponding neuron-like signals on the I - V curves. Each colored I - V curve corresponds to a colored curve of the input signal to memristor.

The laboratory memristor demonstrates different responses to an input signal with a small stochastic spread. Figure 2d shows that, for one curve in Figure 2c, with the yellow curve used as an example, the numerical memristor model yields 10 possible curves (also a yellow color) with a small spread. The I - V curves in Figure 2d illustrate the effect of stochastic switching in the memristor response to the voltage signals of the corresponding amplitudes. Since memristor conductivity is adaptively changed according to the input signal, the memristive device demonstrates the property of plasticity.

There is a threshold value of the amplitude (u_1) of the neuron-like signal at which the memristor state switches at each spike. At high amplitudes of the input signal (u_1), the system enters a state of extreme resistance and does not respond to each spike anymore. The memristive device remains in this state. The switching degree strongly depends on the internal changes in the memristive device related to the interrelated transport phenom-

ena in oxide dielectrics, due to electric potential gradients, ion concentration, and local heating [67,68]. These reasons result in the partial recovery and oxidation of conducting filaments in the oxide film. The corresponding dynamical change in conductivity is limited by the applied voltage and leads to the modulation of the strength of neuron coupling and different types of synchronization. In the course of the study, the optimal coupling strength is $z = j(u_1)$; SR = (0.02–0.06) for 1:1 frequency-locking (Figure 3c) and $z = (0.06–0.095)$ for intermittent synchronization (Figure 3d).

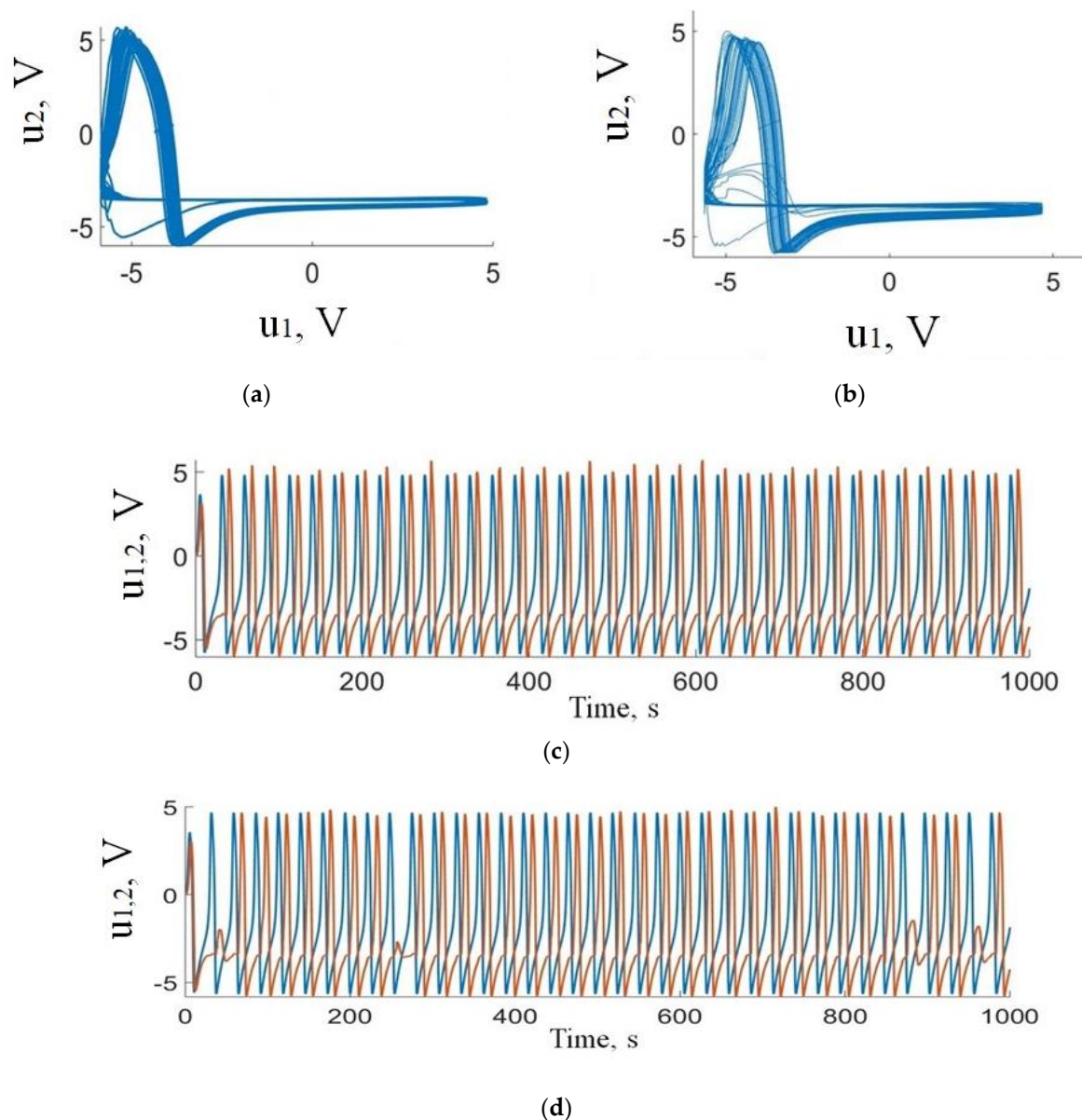


Figure 3. Results of numerical simulations of the dynamics of FHN neuron generators with memristive coupling: (a,b) phase portraits and (c,d) time series representing (a,c) 1:1 and (b,d) intermittent frequency-locking regimes. Blue and red curves show action potentials of presynaptic (u_1) and postsynaptic (u_2) neurons, respectively.

The experiments show that, when the amplitude of the presynaptic neuron u_1 is varied from 1.6 to 2 V, the oscillation frequencies of the coupled neurons are locked either as 2:1 (Figure 4a) or 3:1 (Figure 4b), i.e., the presynaptic neuron u_1 fires the postsynaptic neuron u_2 twice or thrice. This ratio can be randomly changed when chaotic synchronization is reached at higher voltage amplitudes. Although the phase portraits obtained numerically and experimentally do not completely match, the experiment confirms the diversity of

phase-locking regimes predicted by the model. Moreover, our model demonstrates dynamics close to the experimentally observed one, despite of to the first-order memristor model, if the stochasticity of switching is accounted for.

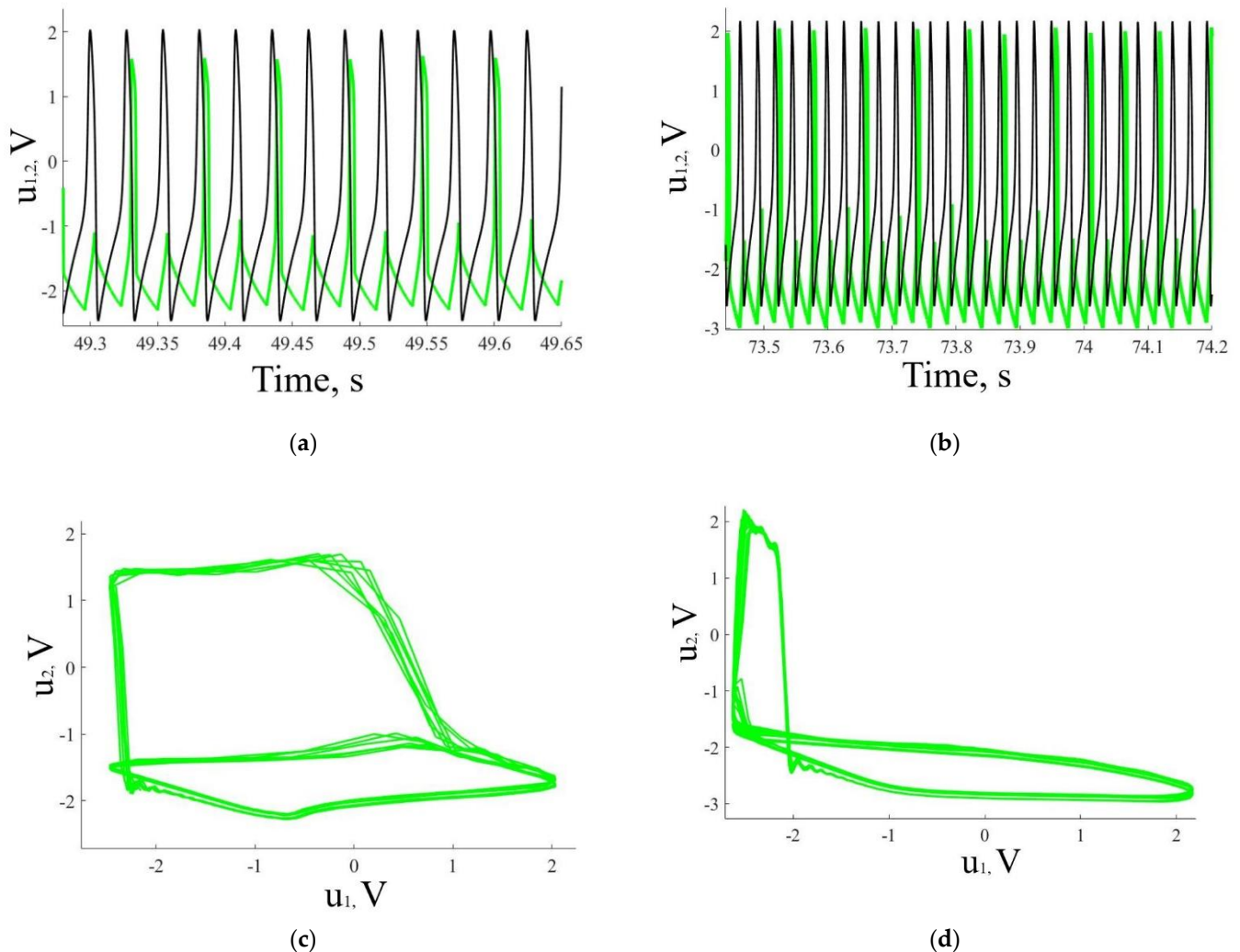


Figure 4. Experimental results demonstrating frequency-locking of FHN electronic neurons coupled by the memristive device: (a,c) time series and (b,d) phase portraits representing (a,b) 2:1 and (c,d) intermittent frequency-locking regimes. Black and green curves show action potential of presynaptic (u_1) and postsynaptic (u_2) neurons, respectively.

The stochasticity is an inalienable property of resistive-switching devices, enabling the so-called stochastic plasticity used to mimic neural synchrony in a simple electronic cognitive system [69]. To the best of our knowledge, the present work is the first attempt to study this important phenomenon both numerically and experimentally. In our case, the stochasticity is modeled through the introduction of fluctuations in the model parameters in a way similar to [70]. Recently, Agudov et al. [71] developed a more generic stochastic model of a memristive device that can be further used to adequately describe the observed complex dynamics of the proposed memristive interface. Another option is to use the deterministic, but at the same time higher-order memristor models based on two or more state variables in order to simulate the experimentally observed intermittency route to chaos [72].

4. Conclusions

In this work, we have studied the dynamics of two coupled FitzHugh–Nagumo neuron generators coupled through a memristive device of a metal–oxide type that adapts

the synaptic connection according to the amplitude of the presynaptic neuron oscillations. The stochastic switching of the memristive device from a high-resistance state to a low-resistance state is achieved by the variation of the internal parameters. Therefore, the memristive synaptic device demonstrates the property of stochastic plasticity. Different synchronous regimes were observed, including 1:1, 2:1, and 3:1 frequency-locking, intermittent synchronization, and more complex dynamics. Its relative compactness and high sensitivity make the proposed neuromemristive device very promising for biorobotics and other bioengineering applications [73].

Author Contributions: Conceptualization, S.A.G. and A.N.P.; methodology, S.A.G. and D.S.K.; software, S.A.G.; validation, S.A.G., A.N.P. and A.N.M.; formal analysis, A.I.B.; investigation, M.N.K. and D.V.G.; resources, A.N.M.; data curation, S.A.G., A.I.B., A.N.P. and A.N.M.; writing—original draft preparation, S.A.G., A.I.B., A.V.L. and V.B.K.; writing—review and editing, M.N.K., A.N.M., V.B.K. and A.N.P.; visualization, S.A.G.; supervision, V.B.K., A.N.M. and A.N.P.; project administration, A.N.M. and A.N.P.; funding acquisition, A.N.M. and A.N.P. All authors have read and agreed to the published version of the manuscript.

Funding: This work was supported by the Russian Science Foundation (Project No. 21-11-00280). A.N.P. acknowledges the Lobachevsky University Competitiveness Program in the frame of the 5-100 Russian Academic Excellence Project.

Institutional Review Board Statement: Not applicable.

Informed Consent Statement: Not applicable.

Data Availability Statement: The data that support the findings of this study are available from the corresponding author upon reasonable request.

Conflicts of Interest: The authors declare no conflict of interest.

References

- Alombah, N.H.; Fotsin, H.; Romanic, K. Coexistence of multiple attractors, metastable chaos and bursting oscillations in a multiscroll memristive chaotic circuit. *Int. J. Bifurc. Chaos* **2017**, *27*, 1750067. [[CrossRef](#)]
- Pikovsky, A.; Rosenblum, M.; Kurths, J. *Synchronization: A Universal Concept in Nonlinear Sciences*; Cambridge University Press: New York, NY, USA, 2001; p. 411.
- Boccaletti, S.; Pisarchik, A.N.; del Genio, C.I.; Amann, A. *Synchronization: From Coupled Systems to Complex Networks*; Cambridge University Press: Cambridge, UK, 2018; p. 255.
- Pisarchik, A.; Jaimes-Reátegui, R.; Sevilla-Escoboza, J.R.; López, J.H.G.; Kazantsev, V. Optical fiber synaptic sensor. *Opt. Lasers Eng.* **2011**, *49*, 736–742. [[CrossRef](#)]
- Pisarchik, A.N.; Sevilla-Escoboza, R.; Jaimes-Reategui, R.; Huerta-Cuellar, G.; García-Lopez, J.H.; Kazantsev, V.B. Experimental implementation of a biometric laser synaptic sensor. *Sensors* **2013**, *13*, 17322–17331. [[CrossRef](#)]
- Simonov, A.Y.; Gordleeva, S.Y.; Pisarchik, A.; Kazantsev, V.B. Synchronization with an arbitrary phase shift in a pair of synaptically coupled neural oscillators. *JETP Lett.* **2014**, *98*, 632–637. [[CrossRef](#)]
- Gerasimova, S.A.; Gelikonov, G.V.; Pisarchik, A.N.; Kazantsev, V.B. Synchronization of optically coupled neural-like oscillators. *J. Commun. Technol. Electron.* **2015**, *60*, 900–903. [[CrossRef](#)]
- Horch, K.W.; Kipke, D.R. *Neuroprosthetics Theory and Practice*, 2nd ed.; World Scientific: Singapore, 2017; Volume 8, p. 934.
- Gerasimova, S.; Lebedeva, A.; Fedulina, A.; Koryazhkina, M.; Belov, A.; Mishchenko, M.; Matveeva, M.; Guseinov, D.; Mikhaylov, A.; Kazantsev, V.; et al. A neurohybrid memristive system for adaptive stimulation of hippocampus. *Chaos Solitons Fractals* **2021**, *146*, 110804. [[CrossRef](#)]
- Hramov, A.E.; Maksimenko, V.A.; Pisarchik, A.N. Physical principles of brain-computer interfaces and their applications for rehabilitation, robotics and control of human brain states. *Phys. Rep.* **2021**, *918*, 1–133. [[CrossRef](#)]
- Indiveri, G.; Linares-Barranco, B.; Hamilton, T.J.; van Schaik, A.; Etienne-Cummings, R.; Delbruck, T.; Liu, S.-C.; Dudek, P.; Häfliger, P.; Renaud, S.; et al. Neuromorphic silicon neuron circuits. *Front. Neurosci.* **2011**, *5*, 73. [[CrossRef](#)] [[PubMed](#)]
- Kuzum, D.; Yu, S.; Wong, H.-S.P. Synaptic electronics: Materials, devices and applications. *Nanotechnology* **2013**, *24*, 382001. [[CrossRef](#)]
- Bill, J.; Legenstein, R. A compound memristive synapse model for statistical learning through STDP in spiking neural networks. *Front. Neurosci.* **2014**, *8*, 412. [[CrossRef](#)] [[PubMed](#)]
- Zhang, T.; Yin, M.; Lu, X.; Cai, Y.; Yang, Y.; Huang, R. Tolerance of intrinsic device variation in fuzzy restricted Boltzmann machine network based on memristive nano-synapses. *Nano Futur.* **2017**, *1*, 015003. [[CrossRef](#)]
- Nair, M.V.; Muller, L.K.; Indiveri, G. A differential memristive synapse circuit for on-line learning in neuromorphic computing systems. *Nano Futur.* **2017**, *1*, 035003. [[CrossRef](#)]

16. Strukov, D.B. Tightening grip. *Nat. Mater.* **2018**, *17*, 293–295. [[CrossRef](#)]
17. Mikhaylov, A.; Pimashkin, A.; Pigareva, Y.; Gerasimova, S.; Gryaznov, E.; Shchanikov, S.; Zuev, A.; Talanov, M.; Lavrov, I.; Demin, V.; et al. Neurohybrid memristive CMOS-integrated systems for biosensors and neuroprosthetics. *Front. Neurosci.* **2020**, *14*, 358. [[CrossRef](#)]
18. Thomas, A. Memristor-based neural networks. *J. Phys. D Appl. Phys.* **2013**, *46*, 093001. [[CrossRef](#)]
19. Adamatzky, A.; Chua, L.O. *Memristor Networks*; Springer: Cham, Switzerland, 2014; p. 716.
20. Ge, R.; Wu, X.; Kim, M.; Shi, J.; Sonde, S.; Tao, L.; Zhang, Y.; Lee, J.C.; Akinwande, D. Atomristor: Nonvolatile resistance switching in atomic sheets of transition metal Dichalcogenides. *Nano Lett.* **2017**, *18*, 434–441. [[CrossRef](#)]
21. Binczak, S.; Jacquir, S.; Bilbault, J.-M.; Kazantsev, V.B.; Nekorkin, V.I. Experimental study of electrical FitzHugh–Nagumo neurons with modified excitability. *Neural Netw.* **2006**, *19*, 684–693. [[CrossRef](#)] [[PubMed](#)]
22. Shchapin, D. Dynamics of two neuronlike elements with inhibitory feedback. *J. Commun. Technol. Electron.* **2009**, *54*, 175–184. [[CrossRef](#)]
23. Adamchik, D.A.; Matrosov, V.V.; Semyanov, A.V.; Kazantsev, V.B. Model of self-oscillations in a neuron generator under the action of an active medium. *JETP Lett.* **2015**, *102*, 624–627. [[CrossRef](#)]
24. Mishchenko, M.A.; Bolshakov, D.I.; Matrosov, V.V. Instrumental implementation of a neuronlike generator with spiking and bursting dynamics based on a phase-locked loop. *Tech. Phys. Lett.* **2017**, *43*, 596–599. [[CrossRef](#)]
25. Pisarchik, A.N.; Jaimes-Reátegui, R.; García-Vellisca, M.A. Asymmetry in electrical coupling between neurons alters multistable firing behavior. *Chaos: Interdiscip. J. Nonlinear Sci.* **2018**, *28*, 033605. [[CrossRef](#)]
26. Gambuzza, L.V.; Frasca, M.; Fortuna, L.; Ntinis, V.; Vourkas, I.; Sirakoulis, G.C. Memristor crossbar for adaptive synchronization. *IEEE Trans. Circuits Syst. I Regul. Pap.* **2017**, *64*, 2124–2133. [[CrossRef](#)]
27. Guseinov, D.; Tetelbaum, D.; Mikhaylov, A.; Belov, A.; Shenina, M.; Korolev, D.; Antonov, I.; Kasatkin, A.; Gorshkov, O.; Okulich, E.; et al. Filamentary model of bipolar resistive switching in capacitor-like memristive nanostructures on the basis of yttria-stabilised zirconia. *Int. J. Nanotechnol.* **2017**, *14*, 604. [[CrossRef](#)]
28. Matrosov, V.V.; Kazantsev, V.B. Bifurcation mechanisms of regular and chaotic network signaling in brain astrocytes. *Chaos: Interdiscip. J. Nonlinear Sci.* **2011**, *21*, 023103. [[CrossRef](#)] [[PubMed](#)]
29. Matrosov, V.V.; Mishchenko, M.A.; Shalfeev, V.D. Neuron-like dynamics of a phase-locked loop. *Eur. Phys. J. Spéc. Top.* **2013**, *222*, 2399–2405. [[CrossRef](#)]
30. Selyutskiy, Y.D. On auto-oscillations of a plate in flow. In *AIP Conference Proceedings*; AIP Publishing LLC location: Melville, NY, USA, 2017; Volume 1798, p. 20139. [[CrossRef](#)]
31. Sausedo-Solorio, J.; Pisarchik, A. Synchronization of map-based neurons with memory and synaptic delay. *Phys. Lett. A* **2014**, *378*, 2108–2112. [[CrossRef](#)]
32. Sausedo-Solorio, J.M.; Pisarchik, A.N. Synchronization in network motifs of delay-coupled map-based neurons. *Eur. Phys. J. Spéc. Top.* **2017**, *226*, 1911–1920. [[CrossRef](#)]
33. Andreev, A.V.; Frolov, N.S.; Pisarchik, A.N.; Hramov, A.E. Chimera state in complex networks of bistable Hodgkin-Huxley neurons. *Phys. Rev. E* **2019**, *100*, 022224. [[CrossRef](#)] [[PubMed](#)]
34. Andreev, A.V.; Maksimenko, V.A.; Pisarchik, A.N.; Hramov, A.E. Synchronization of interacted spiking neuronal networks with inhibitory coupling. *Chaos Solitons Fractals* **2021**, *146*, 110812. [[CrossRef](#)]
35. Bashkirtseva, I.A.; Ryashko, L.B.; Pisarchik, A.N. Ring of map-based neural oscillators: From order to chaos and back. *Chaos Solitons Fractals* **2020**, *136*, 109830. [[CrossRef](#)]
36. Matveyev, Y.; Egorov, K.V.; Markeev, A.; Zenkevich, A. Resistive switching and synaptic properties of fully atomic layer deposition grown TiN/HfO₂/TiN devices. *J. Appl. Phys.* **2015**, *117*, 044901. [[CrossRef](#)]
37. Shi, Y.; Fong, S.; Wong, H.-S.P.; Kuzum, D. Synaptic devices based on phase-change memory. In *Neuro-Inspired Computing Using Resistive Synaptic Devices*; Springer: Cham, Switzerland, 2017; pp. 19–51.
38. Choi, S.; Tan, S.H.; Li, Z.; Kim, Y.; Choi, C.; Chen, P.-Y.; Yeon, H.; Yu, S.; Kim, J. SiGe epitaxial memory for neuromorphic computing with reproducible high performance based on engineered dislocations. *Nat. Mater.* **2018**, *17*, 335–340. [[CrossRef](#)]
39. Gerasimova, S.A.; Mikhaylov, A.; Belov, A.I.; Korolev, D.; Gorshkov, O.N.; Kazantsev, V.B. Simulation of synaptic coupling of neuron-like generators via a memristive device. *Tech. Phys.* **2017**, *62*, 1259–1265. [[CrossRef](#)]
40. Ignatov, M.; Ziegler, M.; Hansen, M.; Petraru, A.; Kohlstedt, H. A memristive spiking neuron with firing rate coding. *Front. Neurosci.* **2015**, *9*, 376. [[CrossRef](#)] [[PubMed](#)]
41. Korotkov, A.G.; Kazakov, A.; Levanova, T.; Osipov, G.V. The dynamics of ensemble of neuron-like elements with excitatory couplings. *Commun. Nonlinear Sci. Numer. Simul.* **2018**, *71*, 38–49. [[CrossRef](#)]
42. Bao, H.; Zhang, Y.; Liu, W.; Bao, B. Memristor synapse-coupled memristive neuron network: Synchronization transition and occurrence of chimera. *Nonlinear Dyn.* **2020**, *100*, 937–950. [[CrossRef](#)]
43. Parastesh, F.; Jafari, S.; Azarnoush, H.; Hatef, B.; Namazi, H.; Dudkowski, D. Chimera in a network of memristor-based Hopfield neural network. *Eur. Phys. J. Spéc. Top.* **2019**, *228*, 2023–2033. [[CrossRef](#)]
44. Pershin, Y.V.; Di Ventra, M. On the validity of memristor modeling in the neural network literature. *Neural Netw.* **2020**, *121*, 52–56. [[CrossRef](#)]
45. Williamson, A.; Schumann, L.; Hiller, L.; Klefenz, F.; Hoerselmann, I.; Husar, P.; Schober, A. Synaptic behavior and STDP of asymmetric nanoscale memristors in biohybrid systems. *Nanoscale* **2013**, *5*, 7297–7303. [[CrossRef](#)]

46. Yang, R.; Huang, H.-M.; Hong, Q.-H.; Yin, X.-B.; Tan, Z.-H.; Shi, T.; Zhou, Y.-X.; Miao, X.-S.; Wang, X.-P.; Mi, S.-B.; et al. Synaptic suppression triplet-STDP learning rule realized in second-order memristors. *Adv. Funct. Mater.* **2017**, *28*. [[CrossRef](#)]
47. Serrano-Gotarredona, T.; Masquelier, T.; Prodromakis, T.; Indiveri, G.; Linares-Barranco, B. STDP and STDP variations with memristors for spiking neuromorphic learning systems. *Front. Neurosci.* **2013**, *7*, 2. [[CrossRef](#)] [[PubMed](#)]
48. Nikiruy, K.E.; Surazhevsky, I.A.; Demin, V.A.; Emelyanov, A.V. Spike-timing-dependent and spike-shape-independent plasticities with dopamine-like modulation in nanocomposite memristive synapses. *Phys. Status Solidi A* **2020**, *217*, 1900938. [[CrossRef](#)]
49. Prudnikov, N.V.; Lapkin, D.A.; Emelyanov, A.V.; Minnekhanov, A.A.; Malakhova, Y.N.; Chvalun, S.N.; Demin, V.A.; Erokhin, V.V. Associative STDP-like learning of neuromorphic circuits based on polyaniline memristive microdevices. *J. Phys. D Appl. Phys.* **2020**, *53*, 414001. [[CrossRef](#)]
50. Demin, V.; Nekhaev, D.; Surazhevsky, I.; Nikiruy, K.; Emelyanov, A.; Nikolaev, S.; Rylkov, V.; Kovalchuk, M. Necessary conditions for STDP-based pattern recognition learning in a memristive spiking neural network. *Neural Netw.* **2020**, *134*, 64–75. [[CrossRef](#)]
51. Sarmiento-Reyes, A.; Rodriguez-Velasquez, Y. Maze-solving with a memristive grid of charge-controlled memristors. In Proceedings of the 2018 IEEE 9th Latin American Symposium on Circuits & Systems (LASCAS), Puerto Vallarta, Mexico, 25–28 February 2018; pp. 1–4. [[CrossRef](#)]
52. Isah, A.; Nguetcho, A.T.; Binczak, S.; Bilbault, J. Dynamics of a charge-controlled memristor in master–slave coupling. *Electronics* **2020**, *56*, 211–213. [[CrossRef](#)]
53. Raj, P.M.P.; Kalita, A.R.; Kundu, S. Memristive computational amplifiers and equation solvers. In *Modelling, Simulation and Intelligent Computing*; Goel, N., Ed.; Springer Nature: Singapore, 2020; pp. 74–82. [[CrossRef](#)]
54. Guo, T.; Wang, L.; Zhou, M.; Duan, S. A multi-layer memristive recurrent neural network for solving static and dynamic image associative memory. *Neurocomputing* **2018**, *334*, 35–43. [[CrossRef](#)]
55. Tanaka, G.; Nakane, R.; Yamane, T.; Takeda, S.; Nakano, D.; Nakagawa, S.; Hirose, A. Waveform classification by memristive reservoir computing. In *International Conference on Neural Information Processing*; Springer: Cham, Switzerland, 2017; pp. 457–465.
56. Erokhin, V. Memristive Devices for neuromorphic applications: Comparative analysis. *BioNanoScience* **2020**, *10*, 834–847. [[CrossRef](#)]
57. Isah, A.; Nguetcho, A.S.T.; Binczak, S.; Bilbault, J. Memristor dynamics involved in cells communication for a 2D non-linear network. *IET Signal Process.* **2020**, *14*, 427–434. [[CrossRef](#)]
58. Chakma, G.; Adnan, M.; Wyer, A.R.; Weiss, R.; Schuman, C.D.; Rose, G.S. Memristive mixed-signal neuromorphic systems: Energy-efficient learning at the circuit-level. *IEEE J. Emerg. Sel. Top. Circuits Syst.* **2017**, *8*, 125–136. [[CrossRef](#)]
59. Battistoni, S.; Cocuzza, M.; Marasso, S.L.; Verna, A.; Erokhin, V. The role of the internal capacitance in organic memristive device for neuromorphic and sensing applications. *Adv. Electron. Mater.* **2021**, 2100494. [[CrossRef](#)]
60. Bian, H.; Goh, Y.Y.; Liu, Y.; Ling, H.; Xie, L.; Liu, X. Stimuli-responsive memristive materials for artificial synapses and neuromorphic computing. *Adv. Mater.* **2021**, 2006469. [[CrossRef](#)] [[PubMed](#)]
61. Alsuwian, T.; Kousar, F.; Rasheed, U.; Imran, M.; Hussain, F.; Khalil, R.A.; Algadi, H.; Batoool, N.; Khera, E.A.; Kiran, S.; et al. First principles investigation of physically conductive bridge filament formation of aluminum doped perovskite materials for neuromorphic memristive applications. *Chaos Solitons Fractals* **2021**, *150*, 111111. [[CrossRef](#)]
62. Gerasimova, S.A.; Mikhaylov, A.N.; Belov, A.I.; Korolev, D.; Guseinov, D.V.; Lebedeva, A.V.; Gorshkov, O.N.; Kazantsev, V.B. Design of memristive interface between electronic neurons. In *AIP Conference Proceedings*; AIP Publishing LLC location: Melville, NY, USA, 2018; Volume 1959, p. 090005. [[CrossRef](#)]
63. Kasdin, N.J. Runge-Kutta Algorithm for the numerical integration of stochastic differential equations. *J. Guid. Control. Dyn.* **1995**, *18*, 114–120. [[CrossRef](#)]
64. Kasdin, N.J. Discrete simulation of colored noise and stochastic processes and $1/f\alpha$ power law noise generation. *Proc. IEEE* **1995**, *83*, 802–827. [[CrossRef](#)]
65. Higham, D.J. An Algorithmic Introduction to numerical simulation of stochastic differential equations. *SIAM Rev.* **2001**, *43*, 525–546. [[CrossRef](#)]
66. Emelyanov, A.; Nikiruy, K.; Demin, V.; Rylkov, V.; Belov, A.; Korolev, D.; Gryaznov, E.; Pavlov, D.; Gorshkov, O.; Mikhaylov, A.; et al. Yttria-stabilized zirconia cross-point memristive devices for neuromorphic applications. *Microelectron. Eng.* **2019**, *215*, 110988. [[CrossRef](#)]
67. Pan, F.; Gao, S.; Chen, C.; Song, C.; Zeng, F. Recent progress in resistive random access memories: Materials, switching mechanisms, and performance. *Mater. Sci. Eng. R Rep.* **2014**, *83*, 1–59. [[CrossRef](#)]
68. Lee, J.S.; Lee, S.; Noh, T.W. Resistive switching phenomena: A review of statistical physics approaches. *Appl. Phys. Rev.* **2015**, *2*, 031303. [[CrossRef](#)]
69. Ignatov, M.; Ziegler, M.; Hansen, M.; Kohlstedt, H. Memristive stochastic plasticity enables mimicking of neural synchrony: Memristive circuit emulates an optical illusion. *Sci. Adv.* **2017**, *3*, e1700849. [[CrossRef](#)]
70. Miranda, E.; Mehonic, A.; Ng, W.H.; Kenyon, A. Simulation of cycle-to-cycle Instabilities in SiOx-based ReRAM devices using a self-correlated process with long-term variation. *IEEE Electron Device Lett.* **2018**, *40*, 28–31. [[CrossRef](#)]
71. Agudov, N.; Dubkov, A.; Safonov, A.; Krichigin, A.; Kharcheva, A.; Guseinov, D.; Koryazhkina, M.; Novikov, A.; Shishmakova, V.; Antonov, I.; et al. Stochastic model of memristor based on the length of conductive region. *Chaos Solitons Fractals* **2021**, *150*, 111131. [[CrossRef](#)]

-
72. Guseinov, D.; Matyushkin, I.; Chernyaev, N.; Mikhaylov, A.; Pershin, Y. Capacitive effects can make memristors chaotic. *Chaos Solitons Fractals* **2021**, *144*, 110699. [[CrossRef](#)]
 73. Parvizi-Fard, A.; Amiri, M.; Kumar, D.; Iskarous, M.M.; Thakor, N.V. A functional spiking neuronal network for tactile sensing pathway to process edge orientation. *Sci. Rep.* **2021**, *11*, 1320. [[CrossRef](#)] [[PubMed](#)]